A postsynaptic transient K^+ current modulated by arachidonic acid regulates synaptic integration and threshold for LTP induction in hippocampal pyramidal cells

Geert M. J. Ramakers* and Johan F. Storm†

Institute of Physiology, University of Oslo, 0317 Oslo, Norway

Edited by Per O. Andersen, University of Oslo, Oslo, Norway, and approved May 28, 2002 (received for review November 21, 2001)

Voltage-gated ion channels in the dendrites and somata of central neurons can modulate the impact of synaptic inputs. One of the ionic currents contributing to such modulation is the fast inactivating A-type potassium current (I_A). We have investigated the role of I_A in synaptic integration in rat CA1 pyramidal cells by using arachidonic acid (AA) and heteropodatoxin-3 (HpTX3), a selective blocker of the Kv4 channels underlying much of the somatodendritic I_A. AA and HpTX3 each reduced I_A by 60–70% (measured at the soma) and strongly enhanced the amplitude and summation of excitatory postsynaptic responses, thus facilitating action potential discharges. HpTX3 also reduced the threshold for induction of long-term potentiation. We conclude that the postsynaptic I_A is activated during synaptic depolarizations and effectively regulates the somatodendritic integration of high-frequency trains of synaptic input. AA, which can be released by such input, enhances synaptic efficacy by suppressing I_A, which could play an important role in frequency-dependent synaptic plasticity in the hippocampus.

Arachidonic acid (AA) and its metabolic products are important second messengers that can modulate a variety of ion channels (1). In the hippocampus, early evidence indicated that AA may play a role in *N*-methyl-D-aspartate (NMDA) receptor-dependent long-term potentiation (LTP) (2–4). Initially, AA was suggested to act as a retrograde messenger during induction of LTP and AA was found to be released by high-frequency stimulation (5, 6) by way of activation of NMDA receptors (7). However, AA failed to induce the predicted enhancement of glutamate release reliably (8), weakening the retrograde messenger hypothesis (9). Nevertheless, previous results indicate that AA can facilitate LTP induction (4, 5, 8), suggesting that other mechanisms may be involved.

In hippocampal CA1 pyramidal cells, the apical dendrites express a high density of fast-inactivating K^+ channels underlying the transient K^+ current I_A (10). AA suppresses Kv4-mediated I_A in vertebrate neurons and expression systems (11–15), and the dendritic I_A is down-regulated by AA and by means of phosphorylation by protein kinases A and C (12, 16). Because I_A can regulate dendritic excitability (10, 17), these findings raise the possibility that AA, released by high-frequency activation of glutamatergic synapses, can enhance the impact of excitatory postsynaptic potentials (EPSPs) by inhibiting I_A. If such modulation occurs, it would provide a positive feedback regulation of EPSP burst efficacy.

To test this hypothesis, we compared the effects of AA and its nonmetabolizable analogue 5,8,11,14-eicosatetraynoic acid (ETYA), with those of a spider toxin, heteropodatoxin-3 (HpTX3), which selectively suppresses the Kv4-mediated I_A (18). We find that AA, ETYA, and HpTX3 increase the amplitude of individual EPSPs and the temporal summation and charge transfer to the soma of synaptic responses during high-frequency trains of synaptic activation. Furthermore, HpTX3 reduces the threshold for LTP induction in response to weak tetanic stimulation by enhancing the resulting postsynaptic depolarization. These findings strongly suggest that the somatodendritic I_A attenuates the summation of high-frequency trains of EPSPs, thus reducing their somatic impact, and that modulation of this current could be an important gain in control for synaptic communication and plasticity.

Materials and Methods

Hippocampal slices (400 μm thick) were prepared from male Wistar rats (17–35 days) by using a vibratome (Campden Instruments, Loughsborough, U.K.). The slices were superfused with extracellular medium containing 125 mM NaCl, 25 mM $NaHCO_3$, 1.25 mM KCl, 1.25 mM KH_2PO_4, 2 mM $CaCl_2$, 1.5 mM $MgCl_2$, and 16 mM glucose, saturated with 95% O_2/5% CO_2 at 21–22°C.

Whole-cell patch-clamp recordings were obtained from CA1 pyramidal cells (19) by using an Axopatch 1D amplifier (Axon Instruments, Foster City, CA) and the signals were filtered at 2 kHz (−3 dB). Patch pipettes (open pipette resistance, 4–7 MΩ) were filled with a solution containing 140 mM K-gluconate or 140 mM Cs-gluconate, 10 mM Hepes, 2 mM ATP, 0.4 mM GTP, 2 mM $MgCl_2$, 5 mM glutathione, 11 mM EGTA, and 1 mM $CaCl_2$. The series-resistance (12–26 MΩ) was compensated (>80%), and all potentials were corrected for the junction potential (−10 mV). All recordings included in this study are from cells with a resting membrane potential < -60 mV and a stable holding potential/series resistance (voltage-clamp) or membrane potential/bridge balance (current-clamp).

Excitatory postsynaptic currents (EPSCs) were recorded in whole-cell voltage-clamp and corresponding potentials (EPSPs) were recorded in whole-cell current-clamp (bridge) mode, with 2 mM extracellular Ca^{2+}. A glass pipette filled with extracellular medium was used to stimulate presynaptic axons in stratum radiatum (monophasic pulses of 100 μs × 15–100 μA from a Hi-Med stimulator, Reading, U.K.). The intracellular free $[Ca^{2+}]$ was buffered at 150 nM with 11 mM EGTA/1 mM Ca^{2+} to prevent induction of NMDA receptor-dependent long-term potentiation or depression. α-Amino-3-hydroxy-5-methylisoxazole receptor-mediated EPSPs/EPSCs were isolated by adding the antagonists L-2-amino-5-phosphonopentanoic acid (100 μM), and bicuculline (10 μM free base) or picrotoxin (0.1 mM).

To record I_A, cells were voltage-clamped at −80 mV in Ca^{2+}-free medium with 2 mM Mn^{2+}, 0.5 μM tetrodotoxin, and

This paper was submitted directly (Track II) to the PNAS office.

Abbreviations: AA, arachidonic acid; 4AP, 4-aminopyridine; EPSC, excitatory postsynaptic current; EPSP, excitatory postsynaptic potential; fEPSP, field excitatory postsynaptic potential; ETYA, 5,8,11,14-eicosatetraynoic acid; HpTX3, heteropodatoxin-3; LTP, long-term potentiation; NMDA, *N*-methyl-D-aspartate; PPF, paired-pulse facilitation.

*Present address: Rudolf Magnus Institute for Neurosciences, UMC Utrecht, Universiteitsweg 100, 3584 CG Utrecht, The Netherlands.

†To whom reprint requests should be addressed. E-mail: j.f.storm@basalmed.uio.no.

www.pnas.org/cgi/doi/10.1073/pnas.152620399

tetraethylammonium (20–30 mM), to block voltage-gated Ca^{2+}, Na^+ and delayed rectifier K^+ channels, and bicuculline (free base; 10 μM) to prevent spontaneous inhibitory postsynaptic currents. The evoked currents were leak-subtracted (P/N protocol, $n = 8$), and I_A was isolated by using a digital subtraction protocol. The sustained current, elicited by a 500- or 250-ms voltage step to +30 or −10 mV preceded by a 100-ms prepulse at 0 or −30 mV, was digitally subtracted from the total outward current during a 500- or 250-ms voltage step to +30 or −10 mV preceded by a 100-ms prepulse at −120 mV. The average current amplitude (step to +30 mV) after subtraction was 3.05 ± 0.18 nA (23.83 ± 1.62 nS, average ± SEM; $n = 18$). Although a precise biophysical characterization of I_A in intact cells is hampered by space-clamp problems (20), the subtracted current closely resembled I_A recorded under better voltage control (13, 17).

Field potentials were recorded at 30°C in the stratum radiatum of CA1 with patch pipettes filled with extracellular medium and an Axoclamp2A amplifier (Axon Instruments). Two monopolar stimulation electrodes (sharpened tungsten wires) were placed in the stratum radiatum of CA1 to stimulate axons both ortho- and antidromically (monophasic pulses, 100 μs, 60–450 μA). The independence of the two stimulated pathways (P1, P2) was tested by a paired-pulse protocol in which P1 and P2 were stimulated at an interval of 50 ms. Only experiments in which there was no facilitation of the second response are included.

Data were digitized by using a DIGIDATA 1200 interface and PCLAMP7 software (Axon Instruments) and stored on videotape (VR10B, Instrutech, Mineola, NY). Data were analyzed and plotted by using CLAMPFIT6 (Axon Instruments) and ORIGIN (Microcal Software, Northampton, MA) software. All averaged data are presented as means ± SEM and were compared by using a Student's t test.

AA (sodium salt; Sigma), HpTX3 (NPS Pharmaceuticals, Salt Lake City, UT), and tetrodotoxin (Alomone Labs, Jerusalem) were dissolved in distilled water, and ETYA (Calbiochem) in ethanol to produce stock solutions (>1,000× concentrated) and added to the external medium (which contained 0.1% BSA when HpTX3 was applied). Stock solutions of AA were used within 14 days because of their instability. L-2-Amino-5-phosphonopentanoic acid was obtained from Tocris Neuramin (Bristol, U.K.); all other chemicals were from Sigma.

Results

AA Enhances Synaptic Potentials and Reduces I_A. To measure the effect of AA and its nonmetabolizable analogue ETYA on synaptic transmission, short series of EPSPs were elicited by trains of five stimuli delivered by an electrode in the stratum radiatum of CA1. In current-clamp recordings, AA (10 μM) and ETYA (5 μM) substantially increased the amplitude of the summed train of EPSPs, thereby eliciting action potentials (Fig. 1*A1* and *A2*). AA also increased the amplitudes of a single EPSP (not shown). Application of 10 μM AA enhanced the slope of the first EPSP in the train by 50.09 ± 17.74% (Fig. 1*A3*; $P < 0.02$, $n = 5$), and 5 μM ETYA caused a similar increase (43.21 ± 3.82%; $n = 4$), which strongly suggests that the effects of AA are not caused by a metabolite of AA. The AA- and ETYA-induced enhancement of the EPSPs occurred in the absence of any detectable change in the cell input resistance or membrane time constant. Furthermore, the paired pulse facilitation (PPF) ratio was not significantly changed during AA (Fig. 1*A4*), indicating that AA did not affect transmitter release probability (21). After AA application, the PPF ratio was 0.92 ± 0.10 times that of the control value (not significant, $n = 5$).

To quantify the effect of AA on the summation of EPSPs before spike discharges we determined the ratio between the slope of the third and the first EPSPs. AA increased this ratio from 1.58 ± 0.09 to 1.87 ± 0.04 ($n = 5$, $P < 0.02$; Fig. 1*B1*), indicating that AA enhanced the EPSP summation. The effects

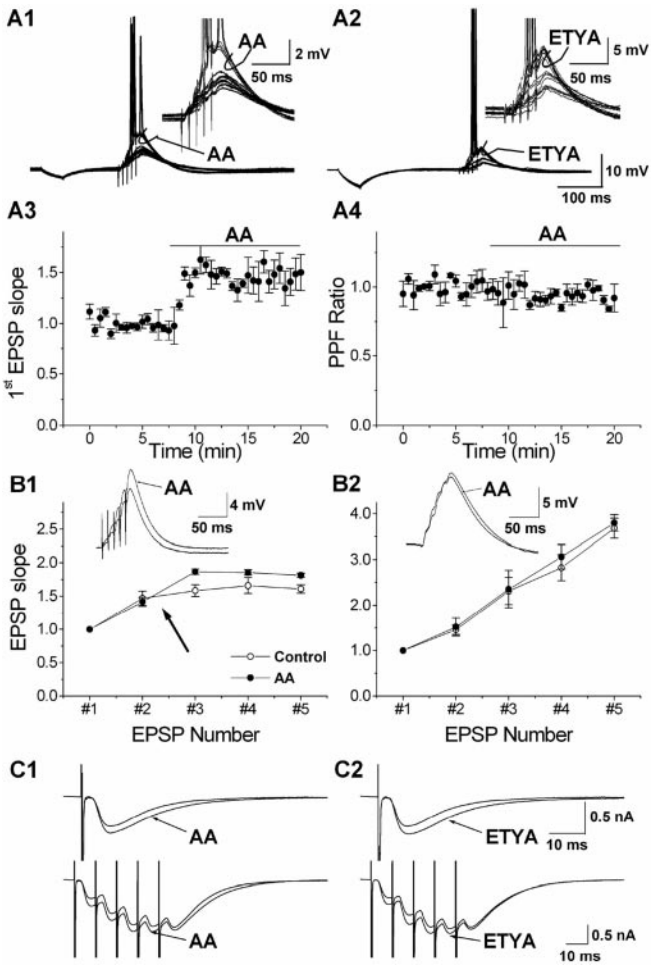

Fig. 1. AA and ETYA increase synaptic responses in CA1 pyramidal cells. (*A*) Typical examples of the effect of 10 μM AA (*A1*) and 5 μM ETYA (*A2*) on a train of EPSPs evoked by synaptic stimuli (five stimuli at 100 Hz). The EPSP train failed to elicit action potentials in control conditions, but was increased beyond the spike threshold during the application of AA and ETYA (curved arrow; see also the enlarged traces in *Right Inset*). Time course of the effect of AA on the slope of the first EPSP (*A3*; $n = 4$). Application of 10 μM AA caused an increase in the slope of the first EPSP, which stabilized after 2.5 min. The normalized PPF ratio (*A4*; EPSP2/EPSP1) was calculated from the same experiments. Application of 10 μM AA resulted in a slight, nonsignificant decrease in the PPF ratio. (*B*) The effect of AA on the EPSP slope (normalized to the first) during a train of five stimuli at 100 Hz, recorded with 140 mM K-gluconate (*B1*, $n = 4$). In control conditions (open circles; before AA application) the EPSP slope increased to 158% at the third EPSP and then leveled off (161% at the fifth EPSP). In the presence of AA (filled circles) the EPSPs were enhanced (to 186% at the third EPSP). With an intracellular medium containing 140 mM Cs-gluconate (*B2*, $n = 4$), the summation of the EPSPs was linear from the first to the fifth EPSP in control conditions (open circles) and AA had no significant effect on the EPSP summation (filled circles). Typical examples of the effect of AA on a train of EPSPs (average of 10 traces) are shown as *Insets*. (*C*) The top traces are typical examples of the effect of 10 μM AA (*C1*) and 5 μM ETYA (*C2*) on a single EPSC (the average of 10 traces), demonstrating that AA and ETYA caused an increase in the EPSC amplitude. The lower traces are typical examples of the effect of 10 μM AA and 5 μM ETYA on EPSCs (average of 10 traces) evoked by a train of synaptic stimuli (five stimuli at 100 Hz). During AA and ETYA the EPSCs increased, most pronounced for the first, second, and third EPSCs.

of AA on EPSPs that are subthreshold for spike generation, in cells recorded with normal intracellular medium, and with 140 mM Cs^+ in the pipette are summarized in Fig. 1*B*. For later EPSPs (fourth and fifth), the slope was smaller than for the third EPSP, although the summed EPSP amplitude continued to

increase during the train, both in control medium and AA. This reduction was probably caused by recruitment of an AA-resistant K^+ current, because blocking K^+ currents with intracellular Cs^+ abolished the effect, allowing the EPSP slopes to increase throughout the train (Fig. 1*B2*). In addition, Cs^+ occluded the effect of AA (Fig. 1*B2*), supporting the idea that AA acts by suppressing postsynaptic K^+ channels.

The effects of AA and ETYA on synaptic integration were also tested in voltage-clamp at a holding potential of −65 mV (Fig. 1 *C1* and *C2*). AA and ETYA both increased the somatic EPSCs in response to a single synaptic stimulus or a train of five stimuli at 100 Hz. The synaptic charge transfer to the soma (i.e., the integral of the five EPSCs) was also enhanced; it increased by 16.91 ± 0.05% for 10 μM AA ($n = 9, P < 0.02$) and by 19.71 ± 0.07% ($n = 5, P < 0.02$) for 5 μM ETYA. The effects of AA and ETYA on synaptic transmission were observed without any detectable change in the holding current, cell input resistance, or PPF ratio, arguing against nonspecific or presynaptic effects of AA. In addition, no increase in charge transfer was seen in cells loaded with Cs^+ ions to block the postsynaptic K^+ channels (data not shown), which further supports the hypothesis that the EPSPs reaching the soma are normally attenuated by shunting of synaptic current through somatodendritic AA-sensitive K^+ channels, and that AA enhances synaptic summation by inhibiting postsynaptic K^+ channels.

One of the possible K^+ currents modulated by AA is I_A. We therefore studied the effects of AA and ETYA on I_A. Outward currents were elicited by voltage-clamp steps to +30 mV by using a prepulse subtraction protocol designed to isolate I_A (see *Materials and Methods*). When bath-applied during whole-cell voltage-clamp recordings from CA1 pyramidal cells, 5 μM AA or 5 μM ETYA substantially reduced the peak amplitude of I_A (Fig. 2 *A1* and *A2*). The average dose–response curve ($n = 4–6$) shows that AA reduced the I_A amplitude with an apparent EC_{50} of 273 nM (Fig. 2*D*). This value is about one fourth of the EC_{50} reported for AA for blockade of I_A in isolated macropatches (≈1 μM) (13). A maximal inhibition of 72.0% was obtained at 2 μM (Fig. 2*D*). Thus, increasing the dose of AA from 2 to 10 μM did not cause any further reduction of I_A as recorded at the soma.

These data show that AA increases the summation of EPSPs by inhibiting a postsynaptic K^+ conductance, possibly I_A.

HpTX3 Reduces I_A and Increases Postsynaptic Potentials. To test the idea that I_A modulates synaptic signal integration in a more direct manner, we used HpTX3 (18), a peptide from the venom of the spider *Heteropoda venatoria* that blocks K^+ channels of the Kv4 family with considerable specificity. Application of 25 nM HpTX3 clearly reduced the amplitude of I_A (Fig. 2*B*), but had no measurable effect on the holding current at −80 mV, the tetraethylammonium-insensitive sustained current (not shown), or inactivation kinetics (not shown). When applied in cumulatively increasing concentration, HpTX3 blocked the peak current with an apparent EC_{50} of 34.95 nM and a maximal inhibition of 65.4% ($n = 5$; Fig. 2 *C* and *E*). These values are between those obtained for HpTX3 block of Kv4.2 channels expressed in *Xenopus* oocytes ($IC_{50} = 67$ nM at 0 mV for HpTX3) and for HpTX2 block of the Kv4.2-mediated I_{to} in heart cells ($IC_{50} = 16$ nM, at −10 mV) (18). As shown in Fig. 2*E*, full effect was obtained between 75 and 100 nM (75 nM HpTX3 reduced I_A by 68.8%, 100 nM HpTX3 by 69.8%).

Having established that HpTX3 efficiently reduces I_A in CA1 pyramidal neurons, we tested its effect on synaptic transmission. HpTX3 substantially enhanced single EPSPs as well as the summed EPSPs in response to trains of stimuli (Fig. 3 *A1* and *A2*). Under control conditions, the high-frequency train of EPSPs showed temporal summation, but remained subthreshold for action potential discharge (with the moderate stimulus intensities we used). In contrast, after application of 100 nM

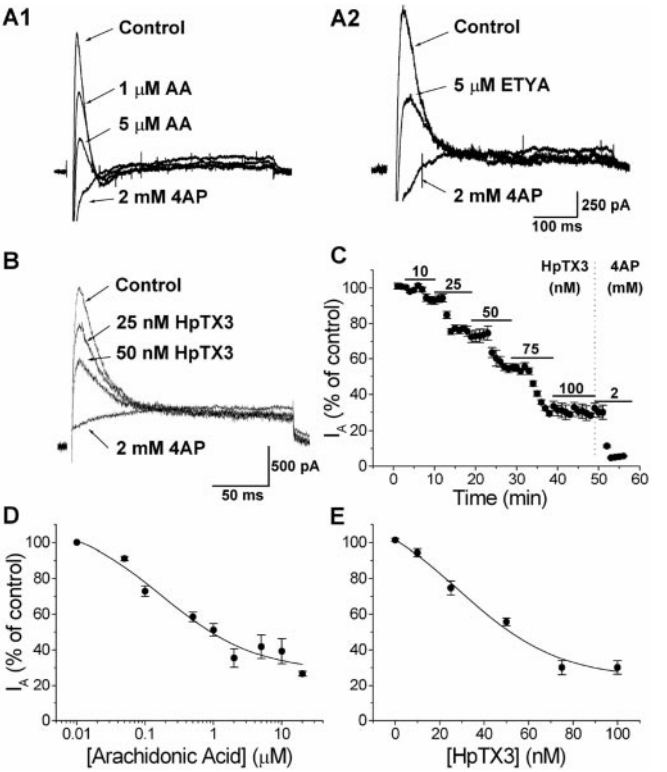

Fig. 2. AA, ETYA, and HpTX3 reduce I_A in CA1 pyramidal cells. (*A*) AA (*A1*; 1 and 5 μM) reduced the amplitude of I_A, which was subsequently fully blocked by 2 mM 4AP. The effect of 5 μM nonmetabolizable AA analogue ETYA and 2 mM 4AP on I_A is shown in *A2*. (*B*) Typical example of the effect of two different concentrations of HpTX3 on I_A recorded in the soma of CA1 cells. Increasing concentrations (25 and 50 nM) of HpTX3 reduced the amplitude of I_A. Subsequent application of 2 mM 4AP blocked I_A completely. (*C*) The effect of cumulatively increasing doses of HpTX3 on the I_A amplitude. Five different concentrations of HpTX3 (10, 25, 50, 75, and 100 nM) were tested ($n = 5$). The maximal effect was obtained between 75 and 100 nM HpTX3, and subsequent application of 2 mM 4AP blocked I_A completely. (*D*) Average dose–response curve ($n = 4–6$) showing that the EC_{50} for AA was 0.27 μM and that the maximal inhibition of I_A was 68%. (*E*) Average dose–response curve ($n = 4$) for the effect of HpTX3 on I_A. The EC_{50} was 34.95 nM, and the maximal inhibition of I_A was 65.4%.

HpTX3, the same train of stimuli elicited EPSPs with about twice the original amplitude, which triggered action potentials after the third or fourth stimulus (Fig. 3*A2*). After application of 100 nM HpTX3, the slope of the first EPSP in the train was increased to 250.15 ± 16.90% of the control value (Fig. 3*B1*; $P < 0.02$, $n = 5$). To quantify the increase in EPSP slope during the train, before spike discharges in all cells, we calculated the ratio between the slopes of the third EPSP and the first EPSP for each train. This ratio was significantly enhanced by HpTX3; it increased from 1.71 ± 0.06 before to 2.08 ± 0.11 after application of 100 nM HpTX3 ($P < 0.02$, $n = 5$), most likely reflecting increased postsynaptic summation of EPSPs. The increase in the EPSP slope from the first to the third EPSP induced by 100 nM HpTX3 was larger than the increase induced by 10 μM AA (the ratio increased to 1.87 ± 0.04 and 2.08 ± 0.11 after 10 μM AA and 100 nM HpTX3, respectively). In one experiment the EPSPs during the HpTX3 application triggered Ca^{2+} spikes, which was never observed with AA.

The HpTX3-induced enhancement of the EPSPs occurred in the absence of any detectable change in the cell input resistance or membrane time constant, as reflected in the voltage response to injection of negative current pulses (Fig. 3*A2*, *Left Inset*). Furthermore, the PPF ratio was not changed during HpTX3

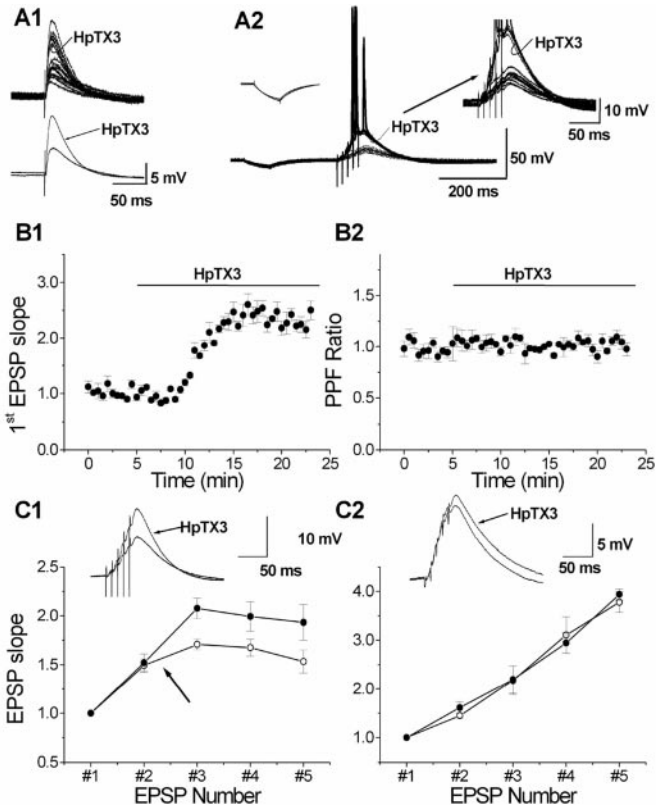

Fig. 3. HpTX3 increases synaptic responses in CA1 pyramidal cells. (*A*) Bath application of 100 nM HpTX3 increased single EPSPs (*A1*). (*Upper*) Individual traces ($n = 10$); (*Lower*) averaged traces. A typical example of the effect of HpTX3 on a train of EPSPs in response to synaptic stimuli (five stimuli at 100 Hz) is shown in *A2*. The EPSPs did not reach threshold for action potential firing in control medium, but were strongly enhanced and triggered action potentials after addition of HpTX3 (curved arrow; see also the enlarged traces in *Right Inset*). *Left Inset* shows that no significant change was induced by HpTX3 in the response to a hyperpolarizing current (100 pA, 50 ms). (*B*) Time course of the effect of HpTX3 on the slope of the first EPSP (*B1*; $n = 5$), normalized to the slope during the control period. The slope was increased by application of 100 nM HpTX3. The normalized PPF ratio (EPSP2/EPSP1) was calculated from the same experiments as shown in *B1*, and application of 100 nM HpTX3 did not change this ratio (*B2*). (*C*) The effect of HpTX3 on the slopes of all five EPSPs (normalized to the slope of the first EPSP) in response to a train of five stimuli at 100 Hz, recorded with 140 mM K-gluconate (*C1*; $n = 5$). In control medium, before HpTX3 application, the EPSP slope increased to 171% at the third EPSP and then declined to 153% at the fifth EPSP. HpTX3 enhanced the increase in the EPSPs, so that the third EPSP slope increased to 208%. However, the relative decline after the third EPSP remained. Typical examples of EPSPs in response to a train of stimuli (five stimuli at 100 Hz) in control conditions and in the presence of 100 nM HpTX3 recorded in whole-cell mode with an internal solution containing 140 mM K-gluconate (K^+) are shown as *Insets*. HpTX3 increased the slope of the first EPSP and the amplitude of the fifth EPSP in the train. Recordings with an intracellular medium with 140 mM Cs-gluconate are shown in *C2* ($n = 4$). The summation of the EPSPs (as determined by the EPSP slope) was linear from the second to the fifth EPSP, no decline occurred after the third EPSP, and HpTX3 had no significant effect on the EPSP summation (unlike in *C1*). Typical examples EPSPs (five stimuli at 100 Hz) in control conditions and in the presence of 100 nM HpTX3 recorded in whole-cell mode with an internal solution containing 140 mM Cs-gluconate are shown as insets. On average HpTX3 did not enhance the EPSPs.

(Fig. 3*B2*), indicating that the toxin did not affect transmitter release probability. Thus, in HpTX3 the PPF ratio was unchanged (103 ± 2% of the control value; not significant, $n = 5$). These observations are in agreement with the hypothesis that I_A in axons within the CA1 field is mainly generated by Kv1.4 subunits, which are HpTX3-insensitive (18), whereas the somatodendritic I_A is primarily caused by the HpTX3-sensitive Kv4 subunits (22, 23).

In three of the five cells tested, action potentials were elicited within 15 min of HpTX3 application and prevented measurement of the maximal amplitude of the summed EPSPs. However, in the two remaining cells and one of the cells that fired spikes after 15 min, the summed EPSP remained subthreshold even after 10 min of HpTX3 application (Fig. 3*C1*). These three cells showed on average a 116% increase in response to 100 nM HpTX3 (peak amplitude, 7.54 ± 0.68 mV in control medium vs. 16.30 ± 1.11 mV after 10 min in HpTX3). Thus, suppression of I_A approximately doubled the EPSP amplitude. To test if the enhancement of the EPSPs by HpTX3 was caused by the blockade of postsynaptic K^+ channels, we used 140 mM Cs^+ in the intracellular medium to suppress postsynaptic K^+ currents. Under these conditions, HpTX3 consistently failed to increase the EPSPs in all cells tested (Fig. 3*C2*; the normalized slope of the fifth EPSP was 3.78 ± 0.21 min before and 3.94 ± 0.11 15 min after HpTX3 application, $n = 4$), which indicates that HpTX3 enhances EPSP summation by blocking somatodendritic K^+ channels. The sharp decline in the EPSP slope increment that was observed after the second EPSP with normal intracellular medium (Fig. 3*C1*, arrow) was not seen in Cs^+-loaded cells, suggesting that this decline was probably due to a HpTX3-resistant K^+ current.

Suppression of I_A Reduces the Threshold for LTP Induction. We next tested whether the increased synaptic integration caused by blockade of I_A reduced the threshold for LTP induction by recording field EPSPs (fEPSPs) in the CA1 stratum radiatum. By using two stimulation electrodes in stratum radiatum, two independent pathways (P1 and P2) were stimulated alternately (30-s intervals). After a stable baseline period of 30 min, one pathway (P1) was given a weak tetanic stimulation (arrow 1 in Fig. 4*A1*), which was subthreshold for LTP induction (a train of 100 stimuli at 50 Hz, at the baseline test intensity, hereafter called a weak tetanus). No change in the slope of the fEPSP was induced. Thirty minutes later, this pathway (P1) was again stimulated with a weak tetanus to ensure that the mere repetition of this stimulation would not change the fEPSP slope (arrow 2 in Fig. 4*A1*; the slope 30 min after the second weak tetanus was 107 ± 0.02% of the baseline value; not significant, $n = 4$). Subsequent application of 100 nM HpTX3 for 60 min (horizontal bar) increased the slope of the fEPSP in both P1 and P2 by 61 ± 0.67% ($P \leq 0.05$, $n = 8$).

In the presence of HpTX3, the other (naive) pathway (P2) was stimulated with a weak tetanus (arrow 3 in Fig. 4*A1*), which gave a tetanus-induced stable potentiation (LTP) of the P2 fEPSP slope (85 ± 0.23% increase, $P \leq 0.05$, $n = 4$; summary time course shown in Fig. 4*B2*). To exclude the possibility that the LTP-inducing effect of a weak tetanus in the presence of HpTX3 was simply caused by the enhanced baseline fEPSP slope, the stimulus intensity of the first pathway (P1) was then reduced (adjusted) to match the slope before HpTX3 application (arrow 4 in Fig. 4*A1*). A weak tetanus delivered to P1 (arrow 5) now produced a stable potentiation also in this pathway (83 ± 0.09% increase in P1, $P \leq 0.05$, $n = 4$; see summary data in Fig. 4*B1*), thus indicating that the potentiation was not due to the enhanced baseline fEPSP slope *per se*.

Although the weak tetanus had no effect on the fEPSPs in control medium, the same weak tetanus delivered in the presence of HpTX3 reliably induced LTP (both in the adjusted pathway, P1, and the nonadjusted pathway, P2). Thus, LTP induction was facilitated by HpTX3; the effect of the weak tetanus was clearly different in the two conditions, $P \leq 0.05$, $n = 4$ (Fig. 4*C*). This conclusion is also supported by the rightward shift of the cumulative probability plot (Fig. 4*D*), which shows the relative change in the slope of the fEPSPs 20–30 min after

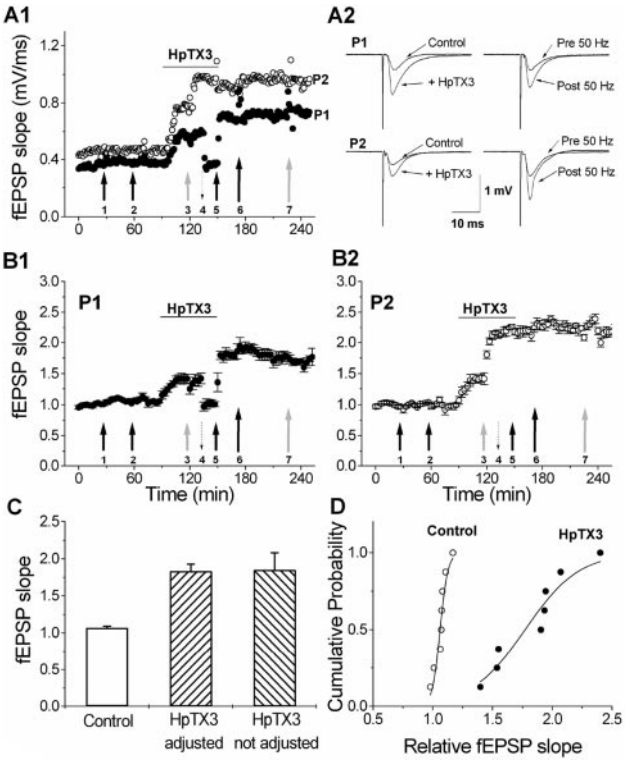

Fig. 4. HpTX3 reduces the threshold for LTP induction. (*A*) Individual experiment in which fEPSPs were elicited in the CA1 field by stimulating two independent pathways (P1 and P2) in stratum radiatum. (*A1*) After a 30-min stable baseline period, a weak tetanus (100 stimuli at 50 Hz test intensity) was applied to one of the pathways, P1 (black arrow 1). This train did not induce any stable potentiation. A second weak tetanus given to P1 (black arrow 2) also failed to change the fEPSP slope. Application of 100 nM HpTX3 (horizontal line) increased the fEPSP slope. After the HpTX3 effect had stabilized, a weak tetanus was delivered to P2 (gray arrow 3), inducing a stable potentiation of the fEPSP slope. Next, the intensity of P1 was reduced to evoke responses of comparable size to before the HpTX3 application (dashed downward arrow 4), and another weak tetanus given to P1 (black arrow 5) that produced stable potentiation. After termination of the HpTX3 application, the fEPSP slopes were not detectably reduced. A strong tetanus (100 Hz for 1 s) given to P1 (long black arrow 6) or P2 (long white arrow 6) did not induce any further potentiation. Sample traces (averages of five sweeps) from this experiment are plotted in *A2*. The profiles on the left illustrate the effect of HpTX3 on the fEPSPs, and the profiles on the right illustrate the effect of the 50-Hz train at adjusted intensity (P1) or test intensity (P2) in the presence of HpTX3. (*B*) *B1* shows the average of four independent experiments for one pathway (P1), in which the stimulus intensity was reduced after HpTX3 had increased synaptic responses (dashed arrow). *B2* shows the average of four independent experiments for the other pathway (P2), in which the stimulus intensity was not changed after HpTX3 had increased synaptic responses. (*C*) Bar graph showing the effect of a weak tetanus (50 Hz for 2 s) measured after 20–30 min. In control conditions ($n = 4$) the fEPSP slope was not changed by the weak tetanus, whereas in the presence of 100 nM HpTX3 the weak tetanus produced an increase in the fEPSP slope. The increase was the same for the pathway that received the train at test intensity (P1, $n = 4$) and the pathway that received the train at reduced intensity (P2, $n = 4$). The effect of the 50-Hz train in the presence of HpTX3 was significantly different from the effect of the 50-Hz train in control conditions ($P \leq 0.05$ for both intensities, Student's *t* test). (*D*) Cumulative probability plot of the effect of a weak tetanus (50 Hz for 2 s) on the fEPSP slope in control conditions ($n = 8$, open circles) and in the presence of 100 nM HpTX3 ($n = 8$, filled circles, data of test and reduced intensity were pooled). In the presence of HpTX3, the 50-Hz train produced a potentiation of the fEPSP slope in all experiments, thus shifting the curve to the right.

the weak tetanus in each individual experiment. In control medium the weak tetanus caused virtually no change in the fEPSP, whereas in the presence of HpTX3 the weak tetanus increased the fEPSP slope in each experiment. Subsequent strong tetanic stimulation (100 Hz; long arrows, marked 6 and 7, in Fig. 4 *A* and *B*) caused no further increase in either pathway, suggesting that the LTP mechanism was already saturated by the weak stimuli in the presence of HpTX. These results indicate that blockade of I_A can critically control the induction of LTP.

Discussion

The primary goal of this study was to elucidate the functional roles of the postsynaptic A-current (I_A) during excitatory synaptic input in CA1 hippocampal pyramidal cells. The biophysical characteristics of I_A in the soma and dendrites of CA1 cells, as well as the effects of AA, ETYA, and HpTX-3 on I_A in neurons and expression systems, have been described (12–15, 17, 18, 23). The main results of the present study are (*i*) that the Kv4 channel blockers AA, ETYA, and HpTX3 each suppress most of the somatodendritic I_A that can be recorded by somatic whole-cell voltage-clamp in these cells; and (*ii*) that the suppression of I_A is accompanied by an increase in the amplitude and temporal summation of synaptic potentials resulting in a reduction of the threshold for LTP induction.

The results show that AA can strongly regulate synaptic integration by means of modulation of I_A, a mechanism that could be particularly important during trains of EPSPs resulting from high-frequency spike bursts. Such high-frequency activity occurs in the hippocampus *in vivo* (24) and facilitates induction of LTP, which is hypothesized to underlie hippocampus-dependent learning and memory (25). The AA effects on synaptic efficacy seem to be fully postsynaptic, because we found no change in PPF and no synaptic enhancement by AA after blocking the postsynaptic K^+ channels with Cs^+. The suppression of I_A by AA would be expected to facilitate the induction of LTP both by enhancing the postsynaptic depolarization during EPSPs, and by facilitating the dendritic back-propagation of action potentials (17, 26–28). Modulation of I_A may also be involved in the increased postsynaptic responsiveness that is seen during LTP, so-called "E-S potentiation" (29). Because the E-S potentiation in the CA1 area is homosynaptic, i.e., specific to the tetanized pathway, it could possibly be partly due to a local suppression of I_A after NMDA receptor-induced AA production (7, 30). However, it is at present not clear how such modulation of I_A could be sustained for long enough to explain persistent E-S potentiation. Because Kv4 channels tend to be concentrated (clustered) in the postsynaptic membrane (31), they are likely to be efficiently regulated by local AA production.

AA and HpTX3 both reduce I_A and increase synaptic integration, suggesting that the effects of AA on synaptic integration are mediated through a down-regulation of I_A. We observed a clear effect of AA on basal synaptic efficacy: the EPSP amplitude and the synaptic charge transfer to the soma were substantially increased both for single synaptic stimuli and high-frequency trains of stimuli. HpTX3 enhanced the EPSP summation more than AA, despite the fact that the two substances seem to have very similar effects on I_A (about 65% inhibition, as recorded at the soma). Effects of AA on non-NMDA glutamate receptors (32) or currents other than I_A may explain this apparent discrepancy. In particular, the AA-induced enhancement of the delayed rectifier current, $I_{K(DR)}$ (12) or M-current I_M (33) will partly substitute for the suppression of I_A. These other effects of AA might also explain why a 10 times higher dose of AA failed to affect synaptic efficacy in a previous study (8).

Blockade of dendritic K^+ channels with high concentrations (6 mM) of the broad spectrum K^+ channel blocker 4-aminopyridine (4AP) increased the excitatory synaptic efficacy in CA1 pyramidal cells (17). Here we show that reduction of I_A with more selective Kv4 channel blockers enhances synaptic integration in these cells, which suggests that the modulation of these channels

by second messenger systems could be important for synaptic plasticity. Our finding that the threshold for LTP induction is reduced by HPTX3 supports this suggestion. The phosphorylation-dependent lowering of the threshold for LTP induction by β-adrenergic receptor activation (34, 35) and the cAMP-dependent enhancement of LTP by dopamine by D1/D5 receptors (36) could be mediated by a phosphorylation of Kv4.2 channels (37) resulting in a decrease of I_A (16, 38). I_A has been shown to be modulated by PKC- and PKA-mediated phosphorylation (16, 39, 40). Because such phosphorylation-dependent regulation of postsynaptic I_A is likely to be "heterosynaptic," induced by modulatory inputs from the brainstem and basal forebrain, it may provide a mechanism for more global, state-dependent modulation. In contrast, we hypothesize that the AA-mediated regulation of synaptic efficacy, demonstrated here, could be "homosynaptic," because of suppression of postsynaptic I_A by local endogenous AA production by glutamatergic synapses.

In conclusion, our results indicate that down-regulation of a postsynaptic transient K^+ current, probably mediated by Kv4 channels, enhances excitatory synaptic efficacy, integration, and plasticity in CA1 pyramidal neurons. The modulation of this current can probably also regulate dendritic back-propagation of action potentials (17) and the induction of synaptic plasticity like LTP. Because the A-channels are expressed ubiquitously, it is likely that this mechanism may be common to many neurons and excitatory synaptic connections in the brain. Our results thus provide direct support for the concept (17, 28, 34, 41), that modulation of postsynaptic K^+ channels can regulate synaptic communication.

We thank Drs. L. Graham, W. H. Gispen, D. Hoffman, H. Hu, T. Lomo, M. Smidt, and A. Villarroel for comments. This work was supported by European Union Research Training Grant BIO4CT975106, the Norwegian Research Council (NFR/MH), and the Nansen, Langfeldt and Odd Fellow foundations.

1. Meves, H. (1994) *Prog. Neurobiol.* **43,** 175–186.
2. Lynch, M. A., Errington, M. L. & Bliss, T. V. (1989) *Neuroscience* **30,** 693–701.
3. Massicotte, G., Oliver, M. W., Lynch, G. & Baudry, M. (1990) *Brain Res.* **537,** 49–53.
4. Drapeau, C., Pellerin, L., Wolfe, L. S. & Avoli, M. (1990) *Neurosci. Lett.* **115,** 286–292.
5. Williams, J. H., Errington, M. L., Lynch, M. A. & Bliss, T. V. (1989) *Nature (London)* **341,** 739–742.
6. Williams, J. H., Errington, M. C., Li, Y. G., Lynch, M. A. & Bliss, T. V. P. (1993) *Semin. Neurosci.* **5,** 149–158.
7. Dumuis, A., Sebben, M., Haynes, L., Pin, J. P. & Bockaert, J. (1988) *Nature (London)* **336,** 68–70.
8. O'Dell, T. J., Hawkins, R. D., Kandel, E. R. & Arancio, O. (1991) *Proc. Natl. Acad. Sci. USA* **88,** 11285–11289.
9. Malenka, R. C. & Nicoll, R. A. (1999) *Science* **285,** 1870–1874.
10. Johnston, D., Hoffman, D. A., Magee, J. C., Poolos, N. P., Watanabe, S., Colbert, C. M. & Migliore, M. (2000) *J. Physiol. (London)* **525,** 75–81.
11. Bittner, K. & Muller, W. (1999) *J. Neurophys.* **82,** 508–511.
12. Colbert, C. M. & Pan, E. (1999) *J. Neurosci.* **19,** 8163–8171.
13. Keros, S. & McBain, C. J. (1997) *J. Neurosci.* **17,** 3476–3487.
14. Villarroel, A. (1993) *FEBS Lett.* **335,** 184–188.
15. Villarroel, A. & Schwarz, T. L. (1996) *J. Neurosci.* **16,** 2522–2532.
16. Hoffman, D. A. & Johnston, D. (1998) *J. Neurosci.* **18,** 3521–3528.
17. Hoffman, D. A., Magee, J. C., Colbert, C. M. & Johnston, D. (1997) *Nature (London)* **387,** 869–875.
18. Sanguinetti, M. C., Johnson, J. H., Hammerland, L. G., Kelbaugh, P. R., Volkmann, R. A., Saccomano, N. A. & Mueller, A. L. (1997) *Mol. Pharmacol.* **51,** 491–498.
19. Pedarzani, P. & Storm, J. F. (1993) *Neuron* **11,** 1023–1035.
20. Spruston, N., Jaffe, D. B., Williams, S. H. & Johnston, D. (1993) *J. Neurophys.* **70,** 781–802.
21. Zucker, R. S. (1989) *Annu. Rev. Neurosci.* **12,** 13–31.
22. Maletic-Savatic, M., Lenn, N. J. & Trimmer, J. S. (1995) *J. Neurosci.* **15,** 3840–3851.
23. Martina, M., Schultz, J. H., Ehmke, H., Monyer, H. & Jonas, P. (1998) *J. Neurosci.* **18,** 8111–8125.
24. Fox, S. E. & Ranck, J. B., Jr. (1981) *Exp. Brain Res.* **41,** 399–410.
25. Bliss, T. V. & Collingridge, G. L. (1993) *Nature (London)* **361,** 31–39.
26. Turner, R. W., Meyers, D. E., Richardson, T. L. & Barker, J. L. (1991) *J. Neurosci.* **11,** 2270–2280.
27. Stuart, G., Spruston, N., Sakmann, B. & Hausser, M. (1997) *Trends Neurosci.* **20,** 125–131.
28. Johnston, D., Hoffman, D. A., Colbert, C. M. & Magee, J. C. (1999) *Curr. Opin. Neurobiol.* **9,** 288–292.
29. Andersen, P., Sundberg, S. H., Sveen, O., Swann, J. W. & Wigstrom, H. (1980) *J. Physiol. (London)* **302,** 463–482.
30. Clements, M. P., Bliss, T. V. & Lynch, M. A. (1991) *Neuroscience* **45,** 379–389.
31. Alonso, G. & Widmer, H. (1997) *Neuroscience* **77,** 617–621.
32. Kovalchuk, Y., Miller, B., Sarantis, M. & Attwell, D. (1994) *Brain Res.* **643,** 287–295.
33. Schweitzer, P., Madamba, S. & Siggins, G. R. (1990) *Nature (London)* **346,** 464–467.
34. Sah, P. & Bekkers, J. M. (1996) *J. Neurosci.* **16,** 4537–4542.
35. Thomas, M. J., Moody, T. D., Makhinson, M. & O'Dell, T. J. (1996) *Neuron* **17,** 475–482.
36. Otmakhova, N. A. & Lisman, J. E. (1996) *J. Neurosci.* **16,** 7478–7486.
37. Anderson, A., Adams, J., Qian, Y., Cook, R., Pfaffinger, P. & Sweatt, J. D. (2000) *J. Biol. Chem.* **275,** 5337–5346.
38. Nakamura, T. Y., Coetzee, W. A., Vega-Saen Zde Miera, E., Artman, M. & Rudy, B. (1997) *Am. J. Physiol.* **273,** H1775–H1786.
39. Murray, K. T., Fahrig, S. A., Deal, K. K., Po, S. S., Hu, N. N., Snyders, D. J., Tamkun, M. M. & Bennett, P. B. (1994) *Circ. Res.* **75,** 999–1005.
40. Lotan, I., Dascal, N., Naor, Z. & Boton, R. (1990) *FEBS Lett.* **267,** 25–28.
41. Lampe, B. J., Gaskill, J. L., Keim, S. C. & Brown, B. S. (1997) *Neurosci. Lett.* **222,** 135–137.